Available online at www.sciencedirect.com
SCIENCE DIRECT®
Journal of Solid State Chemistry 177 (2004) 3423–3432
JOURNAL OF SOLID STATE CHEMISTRY
http://elsevier.com/locate/jssc

Hydrothermal synthesis and structural characterization of a novel cadmium-organic framework

Filipe A. Almeida Paz and Jacek Klinowski*

Department of Chemistry, University of Cambridge, Lensfield Road, Cambridge CB2 1EW, UK

Received 5 February 2004; received in revised form 26 April 2004; accepted 2 May 2004

Available online 20 July 2004

Abstract

A three-dimensional diamondoid cadmium-organic framework, formulated as $[Cd(NDC)(H_2O)]$ (**I**) (where NDC^{2-} = 2,6-naphtalenedicarboxylate), has been hydrothermally synthesized and structurally characterized using single-crystal X-ray diffraction. The hydrothermal synthesis of **I** has been optimized by modifying the composition of the reactive mixture and the temperature programme, so that a highly crystalline and pure homogeneous phase could be obtained. A novel layered structure, formulated as $[Cd_2(NDC)(OH)_2]$, was isolated when the molar ratio of triethylamine exceeds ca. 0.7. Both products have been characterized using powder X-ray diffraction, IR and Raman spectroscopies, and elemental and thermal analyses.

Keywords: Metal-organic frameworks; Coordination polymer; Hydrothermal synthesis; Crystal structure; Thermoanalytical measurements; X-ray powder diffraction; Layered compounds

1. Introduction

The design and synthesis of multi-dimensional metal-organic frameworks (MOFs) has attracted recent attention because of their interesting architectures and wide variety of potential applications [1–8]. Solvothermal synthetic routes to novel MOFs at high temperature and pressure (above 100°C and 1 atm) are difficult and were until recently insufficiently explored [6,9–17]. However, hydrothermal methods offer a number of advantages not reachable by any other synthetic routes, particularly in the case of MOFs. First, the solubility of heavy organic molecules in water can be easily increased under usual experimental conditions [18]. Secondly, these same experimental conditions can, for the majority of the systems, overcome the high activation energies necessary to start nucleation of rare complex thermodynamically metastable phases, which can then be isolated and characterized. Despite these advantages, solvothermal synthesis has the disadvantage of being irreversible, usually driven by fast kinetics of nucleation and crystal growth, which lead to insoluble poorly crystalline powders [7,19]. As X-ray diffraction requires good quality single crystals, in order for the structures of novel MOFs to be determined, the experimental conditions (the temperature programme used for the synthesis and the composition of the reactive mixture) need to be optimized, so that the crystallization limitation can be eliminated.

We have focused our attention on highly crystalline MOFs which simultaneously incorporate traditionally used and novel ligands to this field of crystal engineering [20–25]. In this paper we describe the synthesis and structural characterization of a three-dimensional MOF containing Cd^{2+} and 2,6-naphtalenedicarboxylate (NDC^{2-}) anions, $[Cd(NDC)(H_2O)]$ (**I**), which is very similar to that containing Zn^{2+} cations instead of Cd^{2+}, as described by Min et al. [26]. The hydrothermal conditions for the synthesis of **I** have been optimized: the temperature programme for the reactive period has been systematically changed and an optimal programme selected. Such an approach has been successfully applied to another systems [20,21,25]. Furthermore, since the reactive mixture is a typical ternary system composed of Cd^{2+}, H_2NDC and triethylamine, the composition was

*Corresponding author. Fax: +44-1223-33-63-62.
E-mail address: jk18@cam.ac.uk (J. Klinowski).

0022-4596/$ - see front matter © 2004 Elsevier Inc. All rights reserved.
doi:10.1016/j.jssc.2004.05.022

systematically varied in order to isolate the conditions under which a pure homogeneous phase is synthesized. A new layered compound, $[Cd_2(NDC)(OH)_2]$, was isolated when the concentration of TEA was greater than the stoichiometric amount required for complete deprotonation of H_2NDC.

2. Experimental

2.1. Physical measurements

Elemental analysis for carbon, hydrogen and nitrogen was performed on an Exeter Analytical CE-440 Elemental Analyzer. Samples are combusted under an oxygen atmosphere at 975°C for 1 min with helium used as purge gas. FT–IR spectra were collected from KBr pellets (Aldrich 99% +, FT–IR grade) using a Mattson 4000 spectrometer at the University of Aveiro, Portugal. FT-Raman spectra were measured on a Bruker RFS 100 with a Nd:YAG coherent laser ($\lambda = 1064$ nm) in Aveiro. Scanning electron microscopy images were obtained in Aveiro using a FEG-SEM Hitachi S4100 microscope operating at 25 kV. Samples were prepared by deposition on aluminum sample holders and carbon coating. Thermogravimetric analyses were carried out using a Polymer Laboratories TGA 1500 apparatus, with a heating rate of 5°C/min under a constant nitrogen atmosphere with a flow rate of 25 cm^3/min. Powder X-ray diffraction patterns were measured at ambient temperature using the step counting method (step 0.5°, time 460 s) on a STOE STADI-P high-resolution transmission diffractometer equipped with Ge(111)-monochromated Cu$K\alpha$ radiation ($\lambda = 1.5406$ Å), and a position-sensitive detector covering a 6° 2θ angle (40 kV, 40 mA). Simulated powder patterns were based on single-crystal data, and calculated using the STOE Win XPOW software package [27].

2.2. Synthesis

All reagents were readily available from commercial sources and were used as received without further purification. Syntheses were carried out in PTFE-lined stainless-steel reaction vessels (8 cm^3, filling rate 70%), under autogeneous pressure and static conditions. Compounds proved to be air- and light-stable, and insoluble in water and in organic solvents such as methanol, ethanol, acetone, dichloromethane, toluene, DMSO and chloroform.

2.2.1. Synthesis of $[Cd(NDC)(H_2O)]$ (I)

$Cd(NO_3)_2{\cdot}4H_2O$ (0.313 g, Aldrich), 2,6-naphthalenedicarboxylic acid (H_2NDC, 0.217 g, Aldrich), triethylamine (TEA, 0.189 g, Avocado) and distilled water (ca. 6.0 g) were mixed and stirred thoroughly at ambient temperature for 1 h. The suspension, with a molar composition of 1.01 Cd^{2+}:1.00 H_2NDC:1.86 TEA:334 H_2O was transferred to a Parr Teflon-lined reaction vessel and placed inside a preheated oven at 145°C. The temperature profile used for the synthesis has already been reported [25] and is also given in Supporting Information. The highly crystalline product was collected by vacuum filtration and crystals suitable for single-crystal X-ray analysis were manually separated and preserved in a portion of the autoclave mother liquor. The remaining product was washed with distilled water (ca. 50 cm^3) and absolute ethanol (ca. 3×50 cm^3), and then air-dried at 70°C for further analyses.

Elemental composition found: C 42.00% and H 2.39%. Calculated from single-crystal data: C 41.82% and H 2.34%. TGA data (weight losses) and derivative thermogravimetric peaks (DTG; in italics inside the parenthesis): 220–285°C 5.2% (*255*°C); 375–540°C 57.5% (*479*°C). Selected vibrational (FT-IR and FT-Raman in italics; cm^{-1}): ν (O–H, coordinated water), 3242vs; ν (C–H, aromatic compounds), (*3075* and *3052*); $\nu_{asym}(-CO_2^-)$, 1555vs; ν (=C–H, aromatic compounds), 1536 s; from aromatic compounds with groups capable of donating electrons (e.g., carboxylate groups), 1491 m; $\nu_{sym}(-CO_2^-)$, 1399 vs; δ (O–H···O), 1354 s; ν (C–O), (*1237*); ρ (=C–H, substituted naphthalenes), 1192 m; γ (=C–H, substituted naphthalenes), 931 m and 919 w; δ (C=O), 794 s (*789*); γ (C=O), 680 m (*673*); δ (=C–H, substituted naphthalenes), 642 w; ρ [(C=O)–O], 562 m; γ (=C–H, substituted naphthalenes), 487 m; ν (O–H), 458 m.

2.2.2. Variation of the composition of the reactive mixtures and isolation of the layered $[Cd_2(NDC)(OH)_2]$

Table 1 gives the molar composition for each reactive mixture used to study the region of the ternary diagram (Cd^{2+}, H_2NDC and TEA) which leads to highly pure and crystalline compound **I**. Elemental analyses on carbon and hydrogen are also presented for the 12 isolated products (**I_A**–**I_L**).

TGA data (weight losses) and derivative thermogravimetric peaks (DTG; in italics inside the parenthesis) for the layered $[Cd_2(NDC)(OH)_2]$ structure: 370–534°C 45.3% (*423*°C and *460*°C); 534–600°C 13.4% (*560*°C). Selected vibrational data (FT-IR and FT-Raman in italics; cm^{-1}) for the layered $[Cd_2(NDC)(OH)_2]$ structure: ν (O–H coordinated to Cd^{2+}), 3607 vs; ν (C–H, aromatic compounds), 3061 m and 3030 m (*3054*); overtones and combination bands for substituted naphthalene rings, 1940 w and 1826 w; $\nu_{asym}(-CO_2^-)$, 1605 vs and 1574 vs (*1598*); ν (=C–H, aromatic compounds), 1535 m; from aromatic compounds with groups capable of donating electrons (e.g., carboxylate groups), 1496 m (*1486*); $\nu_{sym}(-CO_2^-)$, 1390 vs and 1357 vs (1395); ν (C–O), (1233); ρ (=C–H, substituted naphthalenes), 1187 m and 1200 m; γ (=C–H, substituted naphthalenes), 927 m and

Table 1
Molar composition for the reactive mixtures and CHN elemental analysis of compounds **L**A to _L

Molar composition					Elemental analysis		
	H_2NDC	Water	Cd^{2+}	TEA	C	H	N
A	1.03	345	1.00	1.88	42.25	2.43	0
B	1.00	659	1.00	2.44	37.29	2.11	0.07
C	1.00	1007	1.02	1.74	41.83	2.45	0.07
D	1.00	1314	1.02	1.92	41.72	2.32	0.07
E	1.00	334	1.02	1.20	45.13	2.49	0.03
F	1.00	334	1.04	2.23	40.02	2.26	0
G	1.00	333	1.01	5.56	30.44	1.73	0
H	1.00	343	1.03	10.12	30.27	1.68	0
I	1.99	649	1.00	3.44	45.29	2.59	0
J	1.00	337	1.52	2.10	40.35	2.23	0.05
K	1.00	315	3.78	1.66	41.98	2.33	0.07
L	1.00	330	9.88	1.78	41.11	2.28	0.05
			Theoretical values for:				
			$[Cd(NDC)(H_2O)]$		41.82	2.34	—
			$[Cd_2(NDC)(OH)_2]$		30.34	1.70	—

917 m; δ (C=O), 789 s and 779 s (*782*); δ (Cd–O–H), 733 s, vb; δ (=C–H, substituted naphthalenes), 643 m; Cd–O–H modes, 627 m and 603 m; ρ [(C=O)–O], 561 m; γ (=C–H, substituted naphthalenes), 467 m; ν(O–H), 452 m; ν(Cd–O), 407 m.

2.3. X-ray crystallography

Suitable single crystals were mounted on a glass fiber using perfluoropolyether oil [28]. Data were collected at 180(2) *K* on a Nonius Kappa charge coupled device (CCD) area-detector diffractometer (Mo$K\alpha$ graphite-monochromated radiation, $\lambda = 0.7107$ Å), equipped with an Oxford Cryosystems cryostream and controlled by the Collect software package [29]. Images were processed using the software packages Denzo and Scalepack [30], and the data were corrected for absorption by using the empirical method employed in Sortav [31,32]. Structures were solved by the direct methods of SHELXS-97 [33], and refined by full-matrix least squares on F^2 using SHELXL-97 [34]. All non-hydrogen atoms were directly located from difference Fourier maps and refined, when possible, with anisotropic displacement parameters. All cavity dimensions were calculated by overlapping rigid spheres with van der Waals radii for each element: O, 1.52 Å; C, 1.7 Å and Cd, 2.2 Å (hydrogen atoms were omitted in all cases for simplicity).

All non-hydrogen atoms have been directly located from difference Fourier maps and refined using anisotropic displacement parameters. Cd(2) and the water molecule [O(21)] are located along the crystallographic two-fold axis. The crystallographically unique H-atom associated with the water molecule was also located from difference Fourier maps, and refined with an independent isotropic displacement parameter and the respective O–H distance restrained to 0.85 Å. Hydrogen atoms attached to carbon were located at their idealized positions using the HFIX 43 instruction in SHELXL [34], and included in the refinement in riding-motion approximation with an isotropic thermal displacement parameter fixed at 1.2 times U_{eq} of the atom to which they are attached. The last difference Fourier map synthesis shows the highest peak (0.490 eÅ^{-3}) located at 0.91 Å from O(142), and the deepest hole (−0.567 eÅ^{-3}) at 0.88 Å from Cd(2).

Crystallographic data (excluding structure factors) for structure **I** have been deposited with the Cambridge Crystallographic Data Centre as supplementary publication no. CCDC-230428. Copies of the data can be obtained free of charge on application to CCDC, 12 Union Road, Cambridge CB2 2EZ, UK [fax: (+44) 1223 336033; E_mail: deposit@ccdc.cam.ac.uk].

3. Results and discussion

3.1. Crystal structure of $[Cd(NDC)(H_2O)]$ (I)

The hydrothermal reaction between cadmium(II) nitrate and H_2NDC yielded, after two days, a highly crystalline, air- and light-stable product composed of colorless plate crystals which have been formulated as $[Cd(NDC)(H_2O)]$ (**I**) on the basis of single-crystal X-ray diffraction (Table 2) and elemental analysis. The structure was identified as being similar to that of an analogous compound which contains Zn^{2+} cations instead of Cd^{2+} as reported by Min et al. [26]. Phase purity and homogeneity of the bulk sample have been further confirmed by a direct comparison between the experimental and the simulated (based on single-crystal data) powder X-ray diffraction patterns (Fig. 1).

Table 2
Crystal data and structure refinement information for **I**

Formula	$C_{12}H_8CdO_5$
Formula weight	344.58
Crystal system	Monoclinic
Space group	*C*2/c
a (Å)	23.5807(13)
b (Å)	6.4275(5)
c (Å)	6.9611(6)
β (deg)	91.394(4)
Volume (Å^3)	1054.75(14)
Z	4
D_c (g cm^{-3})	2.170
μ(Mo*K*α) (mm^{-1})	2.080
F(000)	672
Crystal size (mm)	$0.07 \times 0.05 \times 0.02$
Crystal type	Colorless blocks
θ range	4.10–27.48
Index ranges	$-29 \leqslant h \leqslant 28$
	$-8 \leqslant k \leqslant 8$
	$-9 \leqslant l \leqslant 9$
Reflections collected	3622
Independent reflections	1195 ($R_{int} = 0.0409$)
Final *R* indices [$I > 2\sigma(I)$]	$R_1 = 0.0274$
	w$R_2 = 0.0527$
Final *R* indices	$R_1 = 0.0341$
(all data)	w$R_2 = 0.0545$
Largest diff. peak and hole	0.490 and -0.567 eÅ^{-3}

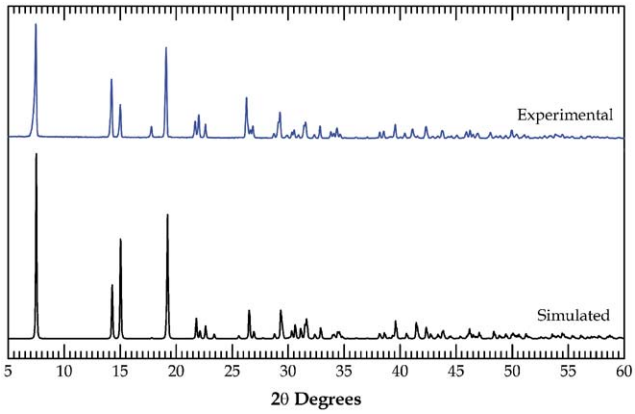

Fig. 1. Simulated and experimental high-resolution (collected in transmission mode) powder X-ray diffraction patterns for **I**.

Compound **I** contains only one crystallographically unique Cd^{2+} site with a distorted square-pyramidal coordination environment, $\{CdO_5\}$ (Fig. 2 and Table 3), composed of four oxygen donor atoms from four different NDC^{2-} ligands (forming the basal plane), and a water molecule occupying the apical position (Fig. 2). Kim et al. have previously reported a Zn–OF in which the metal cations have a similar distorted square-pyramidal coordination environment, but with the NDC^{2-} anionic ligands coordinated in a typical monodentate fashion [35]. The two unique bond lengths of Cd(2) with carboxylate groups are not statistically

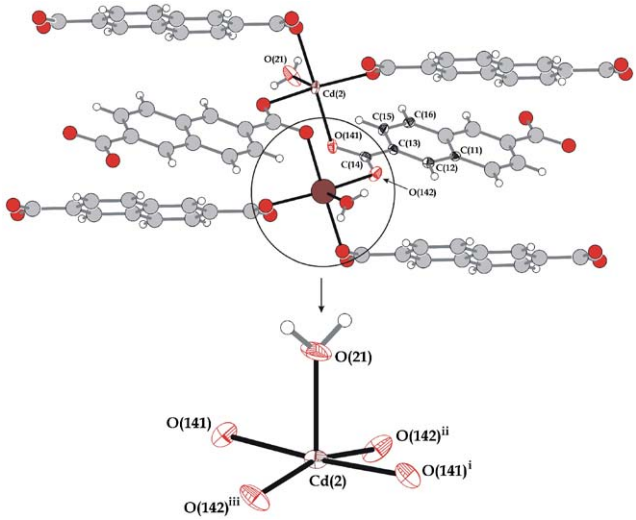

Fig. 2. Schematic representation of (*top*) pseudo-bimetallic repeating structural motif, and (*bottom*) slightly distorted square-pyramidal coordination environment for the crystallographic unique Cd^{2+} metal center in **I**. At the *top*, atoms belonging to the asymmetric unit are represented with thermal ellipsoids drawn at the 50% probability level, and their labeling scheme is also provided. For bond lengths (in Å) and angles (in degrees) see Table 3. Symmetry codes used to generate equivalent atoms: (i) $-x, y, 1/2 - z$; (ii) $x, -y, -1/2 + z$; (iii) $-x, -y, -z$.

identical [Cd(2)–O(141) 2.374(2) Å, and Cd(2)–O(142)^{ii} 2.212(2) Å; symmetry code: (ii) $x, -y, -1/2 + z$], with the average Cd–O bond length of ca. 2.27 Å [including the Cd(2)–O(21) 2.220(3) Å bond length for the coordinated water molecule], which is consistent with values reported for other MOFs [11,26,36,37]. A possible explanation for this arises from the highly asymmetric coordination mode of the C(14) carboxylate group (see below). The same distortions are observed in the coordination environment of the Zn^{2+} metallic center in the analogous compound of **I** [Zn–O 2.189(1) and 1.951(1) Å; Zn–O_{water} 1.974(2) Å] [26].

NDC^{2-} appears in the structure of **I** as an anionic tetradentate bridging ligand (μ_4-NDC; see Fig. 3), acting either as a large spacer [via the naphthalene aromatic ring with Cd(2)$\cdots$Cd(2)^{i} 12.2205(6) Å and Cd(2)$\cdots$Cd(2)^{ii} 12.4281(7) Å; symmetry codes: (i) $1/2 + x, 1/2 + y, +z$; (ii) $1/2 - x, -1/2 - y, -z$] or as a physical bridge between neighboring Cd^{2+} metal centers [via the carboxylate group with Cd(2)$\cdots$Cd(2)^{iii} 4.0439(4) Å; symmetry code: (iii) $-x, 1 - y, -z$]. The C(14) carboxylate group adopts the bidentate *skew–skew*-bridging coordination mode (Fig. 3), with the Cd–O bonds forming angles of ca. 61° [for Cd(2)–O(141)] and ca. 19° [for Cd(2)–O(142)] in respect to the plane of the aromatic ring. The slight differences in comparison with the analogous compound containing Zn^{2+} (ca. 56° and 16°) are attributed to the different effective ionic radii of the two cationic species (for coordination number five, $Cd^{2+} = 0.87$ and $Zn^{2+} = 0.68$ Å) [38] which

Table 3
Selected bond lengths (in Å) and angles (in degrees) for **I**

Cd(2)–O(141)	2.374(2)	O(141)–Cd(2)–O(142)^{iii}	96.45(7)
Cd(2)–O(142)^{ii}	2.212(2)	O(142)^{ii}–Cd(2)–O(141)	84.06(7)
Cd(2)–O(21)	2.220(3)	O(142)^{iii}–Cd(2)–O(141)^{i}	84.06(7)
C(14)–O(141)	1.274(3)	O(21)–Cd(2)–O(141)^{i}	88.05(5)
C(14)–O(142)	1.251(3)	O(21)–Cd(2)–O(142)^{ii}	97.53(6)
		O(21)–Cd(2)–O(141)	88.05(5)
		O(21)–Cd(2)–O(142)^{iii}	97.53(6)
		O(141)–C(14)–O(142)	121.5(3)

Symmetry codes used to generate equivalent atoms: (i) $-x, y, 1/2-z$; (ii) $x, -y, -1/2+z$; (iii) $-x, -y, -z$.

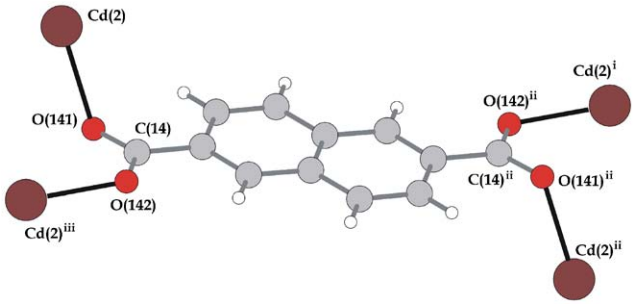

Fig. 3. Schematic representation of the tetradentate coordination pattern for the NDC^{2-} anionic ligands in **I**. Cd(2)···Cd(2)^{i} 12.2205(6) Å; Cd(2)···Cd(2)^{ii} 12.4281(7) Å and Cd(2)···Cd(2)^{iii} 4.0439(4) Å. For selected bond lengths (in Å) and angles (in degrees) see Table 3. Symmetry codes used to generate equivalent atoms: (i) $1/2+x, 1/2+y, +z$; (ii) $1/2-x, -1/2-y, -z$; (iii) $-x, -1-y, -z$.

imposes small distortions in the crystal structures [e.g., the average Zn–O bond length for the analogous compound of **I** is ca. 2.04 Å] [26]. The dihedral angle between the carboxylate group and the naphthalene aromatic ring is almost identical in both compounds (ca. 4° and 5° for **I** and its analogue with Zn^{2+}), clearly indicating the planar nature of this organic spacer. Furthermore, and as expected for bridging carboxylate groups, the O–C–O bite angle is 121.5° and the C–O bonds maintain the equivalence, with the average value of ca. 1.26 Å (Table 3) [39].

Compound **I** has a compact three-dimensional structure (Fig. 4), containing zigzag metallic chains running along the *c* direction of the unit cell and, as previously mentioned, formed by the bridging carboxylate groups (Fig. 3). These chains are interconnected via NDC^{2-} bridges, spaced by small rectangular channels with a cross-section of ca. 2.0×3.5 Å. The coordinated water molecules point towards these channels (Fig. 4b). The solvent molecules are further engaged in two identical hydrogen bonds of medium strength (Table 4) [40], adopting a bifurcated geometry and donating the H–atoms to the O(141) atoms from the nearest carboxylate groups, thus creating a small hydrogen-bonding network [described by a recurring $R_2^2(8)$ graph set] which holds, in the same plane, neighboring zigzag metallic chains (Fig. 5).

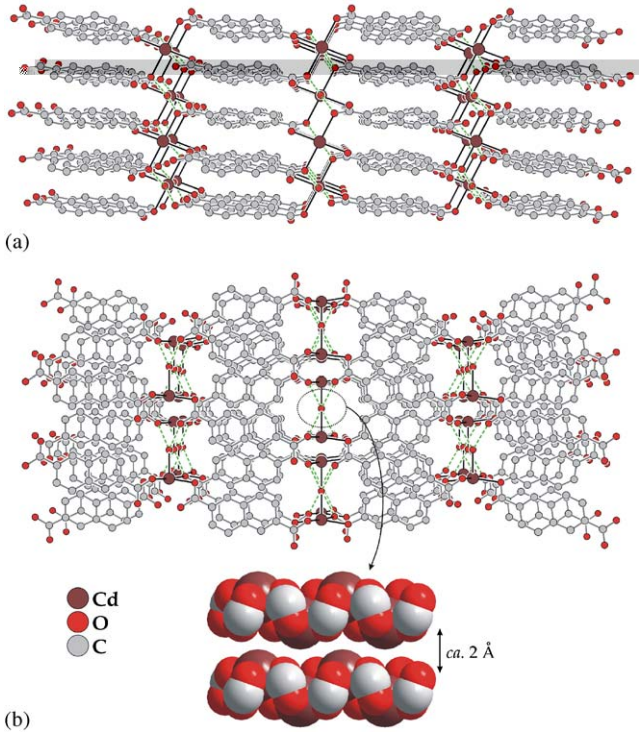

Fig. 4. Crystal packing of **I** along the (a) *b* and (b) *c* directions of the unit cell. The one-dimensional zigzag channel running parallel to the *c* axis and with a cross-section of ca. 2×4 Å, is also represented (at the *bottom*) in space-filling mode. Hydrogen bonds are represented as green-dashed lines (for hydrogen–bonding geometry see Table 4). H–atoms have been omitted for clarity.

Taking the geometrical center between each two consecutive Cd^{2+} cations within the referred metallic chains as nodes for the framework, each node is thus connected to another four, with the smallest closed circuits enclosing a total of six nodes (Fig. 6). Compound **I** can thus be regarded as a distorted (6,4) diamond net containing four nodes inside the unit cell (and the same number of Cd^{2+} cations; Fig. 6b) [41].

3.2. Optimization of the temperature programme

To overcome the limitations of the hydrothermal synthesis, the temperature programme was systematically

Table 4
Hydrogen-bonding geometry for **I** (in Å and degrees)

D–H···A	D(D···A)	< (D–H···A)
O(21)–H(21)···O(241)^{I}	2.676(3)	167(4)

Symmetry code used to generate equivalent atoms: (i) $-x, -y, 1-z$.

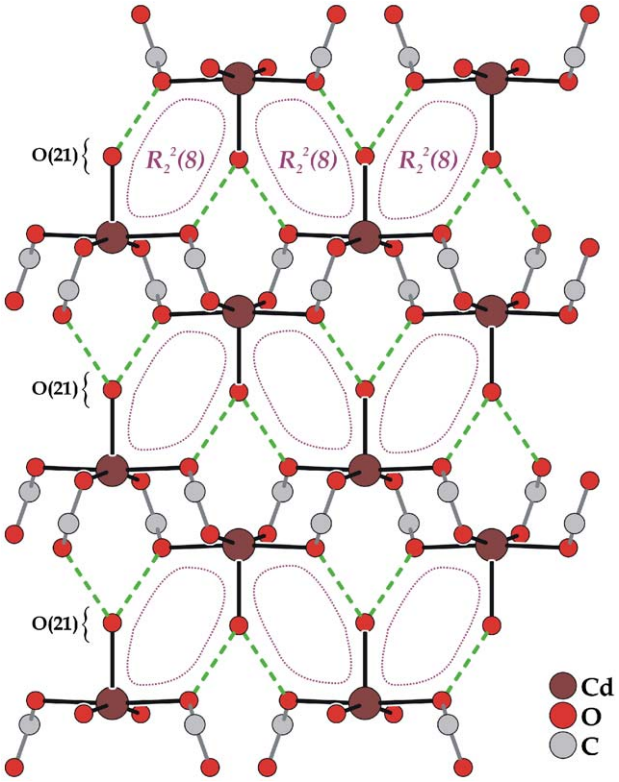

Fig. 5. Perspective view along the *a*-axis showing the hydrogen-bonding network [described by a recurring R_2^2 (8) graph set] which

varied so that an optimal profile could be found [25] (see Supporting Information). The temperature control programme has been progressively optimized taking into account the following: (1) higher temperatures than 145°C were not used due to the high content of organics in the reactive mixtures, and to the fact that it always seems to lead to a mixture of microcrystalline compounds (and probably containing metal oxides); (2) the duration of the reaction at the higher temperature (145°C) has a similar effect to that previously mentioned (formation of a heterogeneous mixture, probably containing metal oxides); (3) post-synthesis quenching of the reaction vessel usually leads to microcrystalline powders; (4) the cooling steps after the reaction at the higher temperature improve the crystallinity of the product, with higher quality single-crystals being obtained when the temperature profile described in Supporting Information is used. In fact, such an approach has already been successfully used to synthesize other MOFs [20,21,25].

3.3. *Variation of the composition of the reactive mixtures*

The composition of the reactive mixture has been systematically changed to identify the chemical ranges which can lead to the synthesis, in high yield (>95%), of highly crystalline **I**. Twelve reactive mixtures (**I**_A to _L; Table 1) with variable amounts of Cd^{2+}, H_2NDC and TEA were prepared, and the products screened using powder X-ray diffraction, IR spectroscopy, elemental and thermal analyses. Fig. 7 shows the ternary diagram with the different molar compositions, along with SEM pictures of selected products.

Fig. 7 and Table 1 show that a variation of the water/Cd^{2+} and Cd^{2+}/H_2NDC ratios for the initial reactive mixtures usually leads to the synthesis of phase-pure **I**, with the only observed differences concerning the level of crystallinity: for high values of the Cd^{2+}/H_2NDC ratio, the formation of large single-crystals is observed; decreasing the water/Cd^{2+} ratio causes a small improvement in the crystallinity of **I**, in this case obtained as a microcrystalline powder.

Mixtures with a concentration of TEA superior to the stoichiometric amount required for a complete deprotonation of H_2NDC produced a different compound, as confirmed by PXRD and IR (Figs. 8 and 9). This new

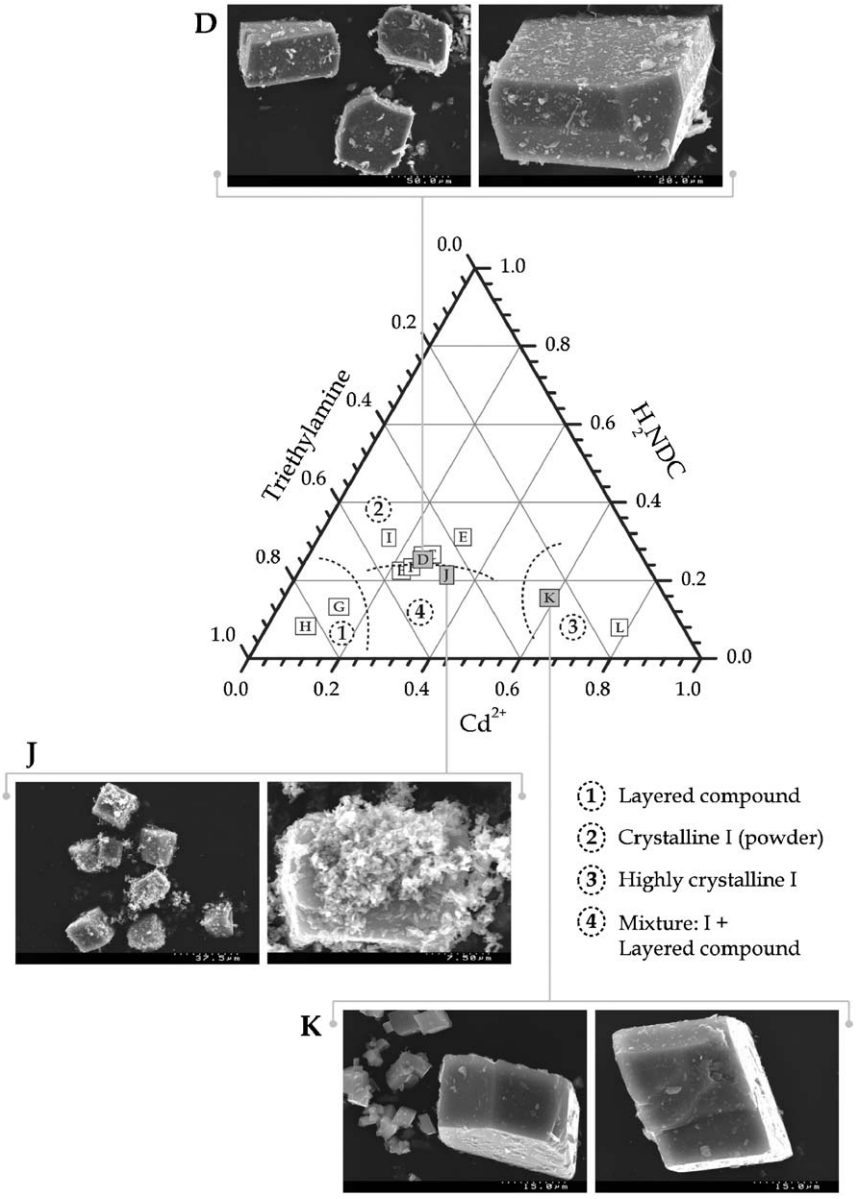

Fig. 7. Ternary diagram for the variation in the composition of the reactive mixture which can lead to compound **I**. Rough estimates of the regions from which compounds **I** and/or $[Cd_2(NDC)(OH)_2]$ (layered) can be isolated are also represented. SEM pictures for selected compounds (**I**_D, **I**_J and **I**_K) are also provided.

structure is layered and was formulated as $[Cd_2(NDC)(OH)_2]$ (see below). We note that **I**_B, _F and _J seem to contain variable amounts of $[Cd_2(NDC)(OH)_2]$ as they are located in the boundary which divides the region dominant for each compound (see Fig. 7). This is markedly observed in the PXRD patterns (the presence of a splitting peak for the first reflection in the patterns of each compound; see Fig. S2 in Supporting Information), IR spectra [e.g., the ν (MO–H) vibrational band; Fig. 9 and Fig. S3 in Supporting Information] and SEM pictures (fine powder surrounding the crystals in Fig. 7).

3.4. Chemical formulation of the layered $[Cd_2(NDC)(OH)]_2$

The isolated compound obtained when the molar ratio of TEA was increased beyond ca. 0.7 (**I**_G and _H in Fig. 7) has been formulated as $[Cd_2(NDC)(OH)_2]$ on the basis of elemental analysis (see Table 1), powder X-ray diffraction, infrared spectroscopy and thermal analysis. The following subsections contain a comparative study between the collected data for **I** and $[Cd_2(NDC)(OH)_2]$, which led to the description of the latter structure.

3.4.1. Powder X-ray diffraction

The PXRD pattern of $[Cd_2(NDC)(OH)_2]$ is typical of a layered structure, with the interlayer separation calculated at ca. 12.46 Å using Bragg's Law (Fig. 8). This separation suggests the presence of NDC^{2-} anions in the interlayer spaces, which probably act as pillars between the layers (Fig. 11).

3.4.2. Thermal analysis

Thermal decomposition of **I** (Fig. 10) proceeds with a first weight loss of 5.2% in the 220–285°C range, consistent with the release of one water molecule per formula unit (5.2% calculated). The second weight loss, of 57.5%, between 375°C and 540°C, is attributed to thermal decomposition of the organic component, leading to the formation of the stoichiometric amount of CdO (37.3% calculated and 37.3% observed residues).

Between ambient temperature and ca. 370°C no weight losses are registered for the layered structure,

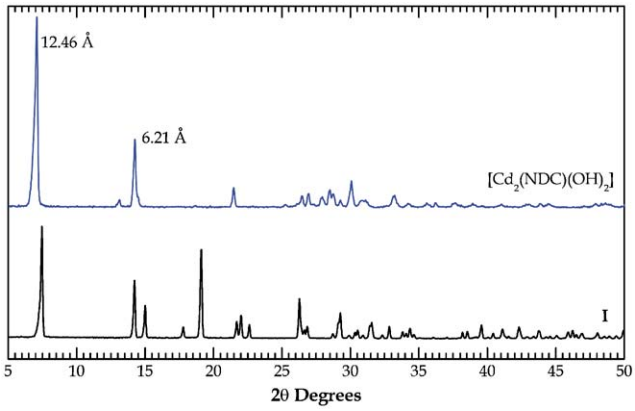

Fig. 8. Powder X-ray diffraction patterns (collected in the transmission mode) for compounds $[Cd_2(NDC)(OH)_2]$ and **I**.

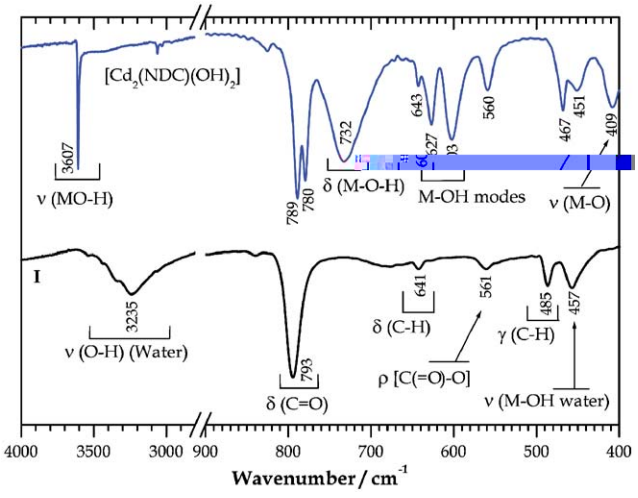

Fig. 9. Selected regions of the IR spectra for compounds $[Cd_2(NDC)(OH)_2]$ and **I**.

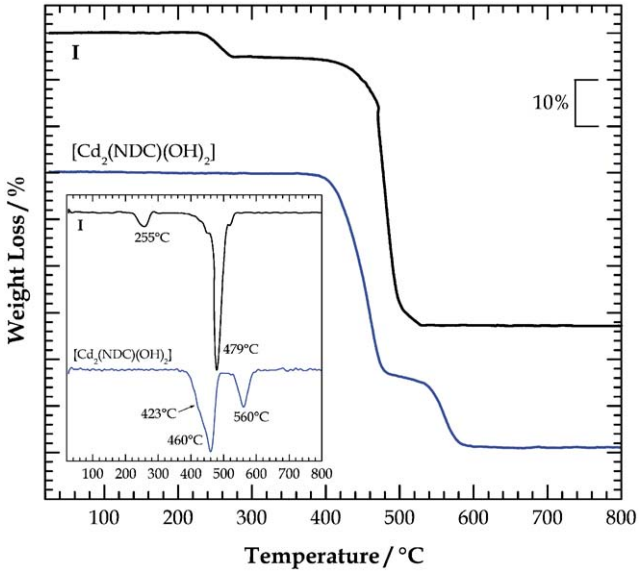

Fig. 10. Thermogravimetric decomposition profiles for compounds **I** and $[Cd_2(NDC)(OH)_2]$ (the inset contains the DTG).

which is a clear indication of the absence of water molecules within the compound (Fig. 10). This, with the CHN elemental analysis values observed for the same compound (Table 1), gave its formulation as $[Cd_2(NDC)(OH)_2]$. In the 370–534°C range, a combined weight loss of 45.3% corresponds, as with **I**, to the total decomposition of the organic component, leading to the formation of CdO (54.3% calculated and 54.7% observed residues). The thermal decomposition continues with a second weight loss of 13.4% in the 534–600°C range. An explanation is well documented [42–44]: at high temperatures and in the presence of reducing agents such as carbon monoxide, CdO starts to sublime, leading to the formation of metallic cadmium (Equations 1 and 2)

$$CdO \xrightarrow{\text{heat} > 400^{\circ}C} Cd(s) + 1/2O_2(g) \quad (1)$$

$$1/2O_2(g) + CO(g) \rightarrow CO_2(g) \quad (2)$$

The sublimation process might have been facilitated by the layered nature of $[Cd_2(NDC)(OH)_2]$, which probably induced the formation of sheet-type CdO fragments with high surface area, which have reacted (in a two-step process as described by Eqs. (1) and (2) with the remaining carbon monoxide from the thermal decomposition of NDC^{2-} (Fig. 11).

3.4.3. Vibrational spectroscopy

IR spectra confirm the presence of 2,6-naphtalenedicarboxylate in both compounds [e.g., through the typical stretching (ν), rocking (ρ), in-plane (δ) and out-of-plane (γ) C–H deformation vibrational modes, and several other modes attributed to carboxylate groups].

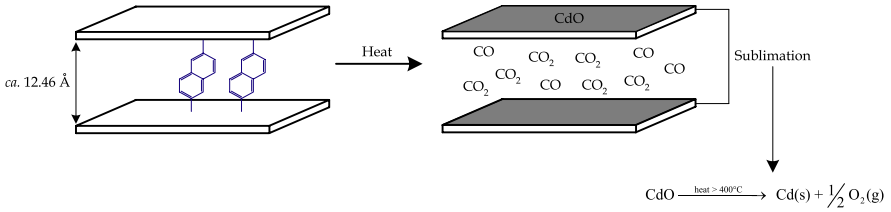

Fig. 11. Schematic representation of the thermal decomposition of $[Cd_2(NDC)(OH)_2]$.

The spectra are particularly informative concerning the presence of an extensive hydrogen-bonding network in **I**, which involves the water molecules [ν (O–H), δ (O–H···O) and γ (O–H···O) vibrational modes], and the absence of such interactions in $[Cd_2(NDC)(OH)_2]$ (see Section 2). Furthermore, a very sharp and strong band centered at $3607\,cm^{-1}$ in the spectra of $[Cd_2(NDC)(OH)_2]$ (Fig. 9) confirms the presence of –OH groups directly bound to the metal centers (other vibrational modes such as the Cd–O–H deformation and the Cd–O stretching are also markedly present in the IR spectrum; see Section 2).

The measured value of $\Delta[\nu_{sym}(-CO_2^-)-\nu_{sym}(-CO_2^-)]$ for **I** ($156\,cm^{-1}$) is typical of a slightly asymmetric chelating coordination mode for the carboxylate group, as revealed by the X-ray diffraction. For $[Cd_2(NDC)(OH)_2]$, the respective Δ values are 248 and $184\,cm^{-1}$, suggesting the presence of carboxylate groups coordinated to the Cd^{2+} centers via the unidentate and the bridging coordination modes, respectively [39,45].

The IR spectrum from $[Cd_2(NDC)(OH)_2]$ does not show the presence of the bands typical of tertiary amines [e.g., δ (C–N–C) in the 510–490 cm^{-1} region] or ammonium salts [e.g., ν (N–H) in the 3350–3050 cm^{-1} region] [46,47]. Consequently, and also considering the elemental analysis composition (Table 1), this further supports the assumption of the absence of TEA molecules in this new layered structure.

4. Conclusions

Based on considerations concerning the composition of the reactive mixture and the temperature programme used for the hydrothermal synthesis, we have demonstrated that the crystalline quality and type of the products obtained when a cadmium salt reacts with 2,6-naphtalenedicarboxylic acid in the presence of triethylamine can be controlled to some extent. In this context, the composition of the ternary reactive mixture has been systematically changed (twelve reactive mixtures have been used) so as to identify the chemical ranges from which a highly crystalline and pure **I** is obtained in high yield (>95%). It was concluded that an increase of the Cd^{2+}/H_2NDC ratio, or a decrease of the water/Cd^{2+} ratio usually induces an increment in the crystallinity. A novel layered structure, formulated as $[Cd_2(NDC)(OH)_2]$, was isolated when the molar ratio of TEA exceeded ca. 0.7. The synthetic assumptions described in this paper have already been confirmed for other reactive systems [20,21,25], and will continue to be the subject of further investigations.

Acknowledgments

We are grateful to the Portuguese Foundation for Science and Technology (FCT) for financial support to F.A.A.P. through the Ph.D. scholarship No. SFRH/BD/3024/2000.

References

[1] S.R. Batten, R. Robson, Angew. Chem. Int. Ed. 37 (1998) 1461.
[2] G.R. Desiraju, Angew. Chem. Int. Ed. Engl. 34 (1995) 2311.
[3] C. Janiak, Dalton Trans. (2003) 2781.
[4] C. Janiak, Angew. Chem. Int. Ed. Engl. 36 (1997) 1431.
[5] S. Kitagawa, M. Kondo, Bull. Chem. Soc. Japan 71 (1998) 1739.
[6] B. Moulton, M.J. Zaworotko, Chem. Rev. 101 (2001) 1629.
[7] M.J. Zaworotko, Chem. Commun. (2001) 1.
[8] O.M. Yaghi, H.L. Li, C. Davis, D. Richardson, T.L. Groy, Acc. Chem. Res. 31 (1998) 474.
[9] Z.Y. Fu, X.T. Wu, J.C. Dai, L.M. Wu, C.P. Cui, S.M. Hu, Chem. Commun. (2001) 1856.
[10] L. Pan, N. Ching, X.Y. Huang, J. Li. Chem. Commun. (2001) 1064.
[11] O.R. Evans, W.B. Lin, Inorg. Chem. 39 (2000) 2189.
[12] S.M.F. Lo, S.S.Y. Chui, L.Y. Shek, Z.Y. Lin, X.X. Zhan, G.H. Wen, I.D. Williams, J. Am. Chem. Soc. 122 (2000) 6293.
[13] J. Tao, M.L. Tong, X.M. Chen. J. Chem. Soc., Dalton Trans. (2000) 3669.
[14] P.J. Hagrman, D. Hagrman, J. Zubieta, Angew. Chem. Int. Ed. 38 (1999) 2639.
[15] J.Y. Lu, M.A. Lawandy, J. Li, T. Yuen, C.L. Lin, Inorg. Chem. 38 (1999) 2695.
[16] Z.Y. Wang, R.G. Xiong, B.M. Foxman, S.R. Wilson, W.B. Lin, Inorg. Chem. 38 (1999) 1523.
[17] Q.M. Wang, G.C. Guo, T.C.W. Mak, Chem. Commun. (1999) 1849.
[18] J. Gopalakrishnan, Chem. Mater. 7 (1995) 1265.
[19] J.C. MacDonald, P.C. Dorrestein, M.M. Pilley, M.M. Foote, J.L. Lundburg, R.W. Henning, A.J. Schultz, J.L. Manson, J. Am. Chem. Soc. 122 (2000) 11692.
[20] F.A.A. Paz, J. Klinowski, J. Phys. Org. Chem. 16 (2003) 772.
[21] F.A.A. Paz, J. Klinowski, Chem. Commun. (2003) 1484.

[22] F.A.A. Paz, A.D. Bond, Y.Z. Khimyak, J. Klinowski, Acta Crystallogr. E 58 (2002) M730.
[23] F.A.A. Paz, A.D. Bond, Y.Z. Khimyak, J. Klinowski, Acta Crystallogr. C 58 (2002) M608.
[24] F.A.A. Paz, A.D. Bond, Y.Z. Khimyak, J. Klinowski, Acta Crystallogr. E 58 (2002) M691.
[25] F.A.A. Paz, Y.Z. Khimyak, A.D. Bond, J. Rocha, J. Klinowski, Eur. J. Inorg. Chem. (2002) 2823.
[26] D. Min, S.S. Yoon, C. Lee, C.Y. Lee, M. Suh, Y.-J. Hwang, W.S. Han, S.W. Lee, Bull. Korean Chem. Soc. 22 (2001) 531.
[27] STOE Win XPOW THEO Version 1.15; STOE & Cie GmbH, 1999.
[28] T. Kottke, D. Stalke, J. Appl. Cryst. 26 (1993) 615.
[29] R. Hooft. Collect: Data Collection Software Nonius B.V. (1998) Delft.
[30] Z. Otwinowski, W. Minor, in: C.W. Carter, R.M. Sweet (Eds.), Methods in Enzymology, Vol. 276, Academic Press, New York, 1997, p. 307.
[31] R.H. Blessing, Acta Crystallogr. A 51 (1995) 33.
[32] R.H. Blessing, J. Appl. Crystallogr. 30 (1997) 421.
[33] G.M. Sheldrick, SHELXS-97, Program for Crystal Structure Solution, University of Göttingen, 1997.
[34] G.M. Sheldrick, SHELXL-97, Program for Crystal Structure Refinement, University of Göttingen, 1997.
[35] J. Kim, B.L. Chen, T.M. Reineke, H.L. Li, M. Eddaoudi, D.B. Moler, M. O'Keeffe, O.M. Yaghi, J. Am. Chem. Soc. 123 (2001) 8239.
[36] G. Yang, H.G. Zhu, B.H. Liang, X.M. Chen, J. Chem. Soc., Dalton Trans. (2001) 580.
[37] E.G. Bakalbassis, M. Korabik, A. Michailides, J. Mrozinski, C. Raptopoulou, S. Skoulika, A. Terzis, D. Tsaousis, J. Chem. Soc., Dalton Trans. (2001) 850.
[38] R.D. Shannon, Acta Crystallogr. A 32 (1976) 751.
[39] C. Oldham, Carboxylates squarates and related species, in: S.G. Wilkinson (Ed.), Comprehensive Coordination Chemistry, Vol. 2, Pergamon, New York, 1987, p. 435.
[40] P. Gilli, V. Bertolasi, V. Ferretti, G. Gilli, J. Am. Chem. Soc. 116 (1994) 909.
[41] A.F. Wells, Structural Inorganic Chemistry, 4th Edition, Oxford University Press, Oxford, 1975.
[42] J.D. Lee, Concise Inorganic Chemistry, 4th Edition, Chapman & Hall, London, 1991.
[43] H. Remy, in: Treatise on Inorganic Chemistry, Vol. 2, Elsevier, Amsterdam, 1956.
[44] M.C. Sneed, R.C. Brasted, in: Comprehensive Inorganic Chemistry, Vol. 4, Van Nostrad, Princeton, NJ, 1955.
[45] G.B. Deacon, R.J. Phillips, Coord. Chem. Rev. 33 (1980) 227.
[46] J.B. Lambert, H.F. Shurvell, D.A. Lightner, R.G. Cooks, Organic Structural Spectroscopy, 1st Edition, Prentice-Hall International (UK) Limited, London, 1998.
[47] N.B. Colthup, L.H. Daly, S.E. Wiberly, Introduction to Infrared and Raman Spectroscopy, 1st Edition, Academic Press Inc, London, 1964.